Modeling of the Hygrothermal Responses of a Sheathing Board in a Prefabricated Wall System and Comparison with Experimental Result

Fitsum Tariku, PhD
Member ASHRAE

Hua Ge, PhD, PEng
Member ASHRAE

ABSTRACT

Drying and wetting can occur locally at different parts of a building envelope and involve simultaneous heat, air, and moisture transfer. These dynamic wetting and drying processes can be captured using advanced hygrothermal models. In this paper, the one-dimensional hygrothermal model HAMFit is used to simulate the dynamic hygrothermal responses of a sheathing board in a prefabricated wall system. The walls comprise the following layers: fiber-cement board as a cladding layer, plywood as a sheathing board, expanded polystyrene (EPS) as insulation, gypsum board as an interior layer, and 6 mil polyethylene sheet as a vapor and air barrier. The simulation results were compared with measured data from an experiment carried out at the field Building Envelope Test Facility, Building Science Centre of Excellence (BSCE), British Columbia Institute of Technology (BCIT). The model's prediction, using the measured indoor and outdoor boundary conditions, of the transient temperature and moisture content of the sheathing board are in good agreement with the experimental data. This paper presents the simulation parameters, including boundary conditions and modeling assumptions.

INTRODUCTION

Drying and wetting can occur locally at different parts of a building envelope and involve simultaneous heat, air, and moisture transfer. These dynamic wetting and drying processes can be captured using advanced hygrothermal models. In various research projects, computer models have been used to assess the performance of a wall system as it is exposed to climatic conditions of different geographical locations (Djebbar et al. 2002; Mukhopadhyaya et al. 2003; Tariku et al. 2007; Maref et al. 2009). They are also used to select appropriate building envelope systems for given geographic locations. These models can generate the transient moisture content and temperature profiles of a chosen location in the computational domain. This information is essential to predicting the likelihood of occurrence of building envelope failure (Tariku et al. 2007). For example, wood-based elements having moisture contents in excess of 20% (wt.) concurrently at temperatures exceeding 10°C would most likely form mold (95% chance) within a period of 90 consecutive days in this condition (Baker 1969; Carll and Highley 1999; Nofal and Morris 2003).

In the last 20 years, various hygrothermal computer models with various degrees of complexities have been developed to assess the long-term moisture and thermal performances of new and existing building envelope components. The relevancy of the model depends on its degree of accuracy in representation of the physical heat, air, and moisture (HAM) transfer phenomena. Analytical and numerical benchmark exercises were developed to test one-dimensional HAM models under a European Union project called HAMSTAD (Hagentoft et al. 2004). Laboratory and field experimental studies (Geving and Uvsløkk 2000; Maref et al. 2002) were also carried out with the objective of generating data for validation of computer models (Tariku and Kumaran 2006). The Building Science Centre of Excellence (BSCE) at the British Columbia Institute of Technology (BCIT) is currently monitoring various wall designs to assess their thermal and moisture performances as well as to generate experimental data for

Fitsum Tariku *is a director of the Building Science Centre of Excellence at the British Columbia Institute of Technology, Burnaby, BC.* ***Hua Ge*** *is an assistant professor in the Department of Architectural Science, Ryerson University, ON.*

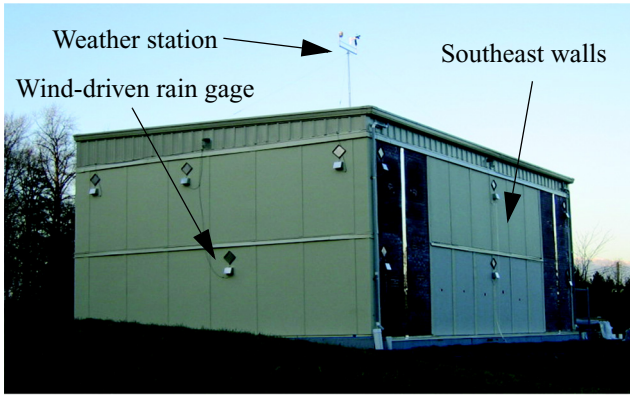

Figure 1 *BCIT's Building Envelope Test Facility (BETF).*

model validations. The intent of this paper is to test and validate the advanced hygrothermal model, HAMFit (Tariku et al. 2010) using field experimental data, including indoor and outdoor boundary conditions and measured temperature and moisture responses of one of the test panels that are being monitored at BCIT's Building Envelope Test Facility (BETF). In this paper, the sheathing board moisture content and temperature responses from March 13 to December 6, 2009 are used for benchmarking the model, and referred in the paper as the monitoring period.

FIELD EXPERIMENT

Test Facility

The experimental study is being carried out at the highly instrumented BCIT Building Envelope Test Facility (BETF) (Figure 1). This unique 44 ft × 28 ft two-story research facility is designed to evaluate the hygrothermal performance of full-scale building envelope assemblies under simulated indoor and real climatic outdoor conditions. The facility is also equipped with a weather station mounted on the rooftop to measure the outdoor boundary conditions, including temperature, relative humidity, wind speed, wind direction, solar radiation on both horizontal and vertical surfaces, and horizontal rainfall. Driving rain on wall surfaces is also collected. More information about this facility can be found in Ge et al. (2008). In this paper, measured indoor and outdoor boundary conditions are used as input data to the computer simulation.

Test Panel

A 4 ft × 8 ft test panel with 16 in. stud spacing was prefabricated and installed in the northwest section of the BETF. The configuration of the 2 in. × 6 in. (38 mm by 140 mm) wood-frame test panel from exterior to interior, in sequence, is as follows: fiber cement board as a cladding layer, two layers of 30-minute-rated asphalt-impregnated building papers as a weather barrier, 12.5 mm plywood as a sheathing board,

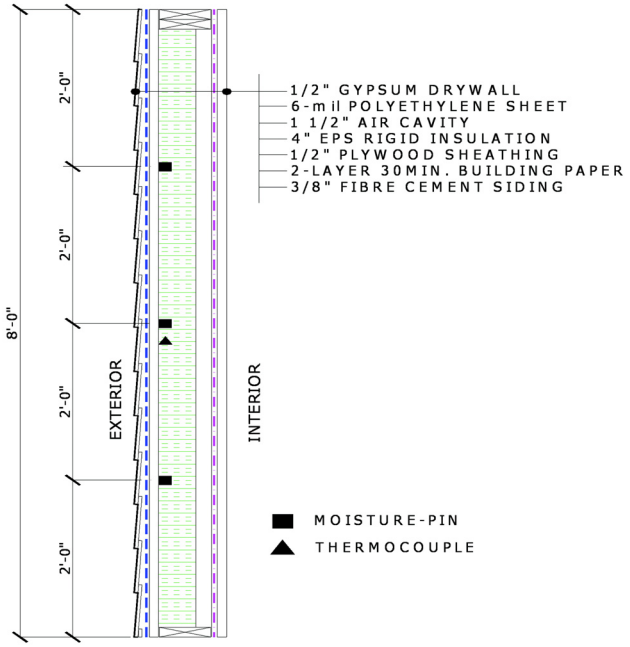

Figure 2 *Vertical cross section of prefabricated wall system considered in the study.*

102 mm expanded polystyrene (EPS), 38 mm airspace, 6 mil polyethylene sheet as a vapor and air barrier, and interior finish (gypsum board, 12.5 mm). The schematic diagram of the vertical cross section of the test panel through the insulation section, along with the corresponding sensors installed to measure the moisture content and temperature of the plywood, is shown in Figure 2.

To measure the moisture contents of the plywood at different heights, three pairs of moisture pins were installed on the test panel from the inside along its center line at the lower, middle, and upper positions (i.e., at one-quarter, half, and three-quarters wall height). The temperature of the plywood was continuously measured with a thermocouple, which was installed at the middle height of the wall. This measurement was also used for conversion of the three electrical resistance measurements to moisture contents.

The core of the test panel, including framing, insulation, polyethylene sheet, and plywood sheathing, was fabricated and instrumented in a controlled environment, and therefore, good workmanship has been achieved (Ge et al. 2009). The building papers, cladding (fiber cement siding), and the interior layer (gypsum board) were installed after the walls were in place on the test facility. To provide the thermal and moisture separation from the surrounding existing walls, the polyethylene sheet was wrapped around the edge of the stud to overlap with the building papers. The gap between test panels was fitted with rigid insulation and sealed to the side with sealant and backing rod.

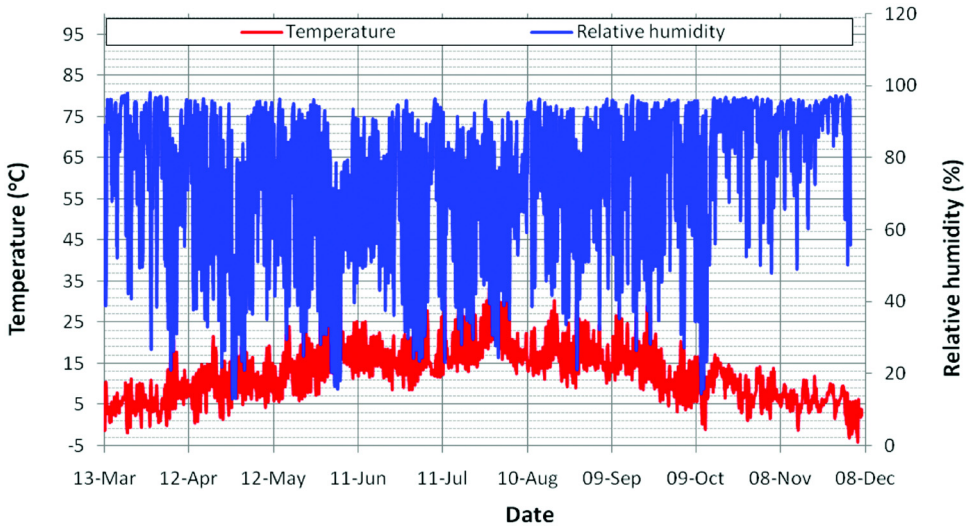

Figure 3 *Daily average outdoor air temperature and relative humidity during the simulation period.*

Indoor and Outdoor Climatic Conditions

During the experimental period, the indoor and outdoor climatic conditions were measured, and then used in the simulation to compute the hourly moisture and heat fluxes on the interior and exterior surfaces of the test panel.

Outdoor Climatic Conditions. The local outdoor climatic conditions, including temperature, relative humidity, wind speed and direction, global solar radiation, and horizontal rainfall, were measured with a weather station mounted on the rooftop of the BETF. The wind-driven rain that impinges the test panel was also measured with a rain gage that was vertically mounted adjacent to the test panel. Figure 3 shows the daily average temperature and relative humidity of the outdoor air during the monitoring period. The hourly average minimum temperature is –4°C and the maximum is 36°C, which occurred on March 13 and July 29, respectively. In general, the outdoor humidity was relatively high in the first and last months of the monitoring period. Figure 4 shows the magnitude and the frequency of wind-driven rain events captured by the wind-drive rain gage adjacent to the test wall. The wind-driven rain loads that the test wall was exposed to were relatively low, in most cases under 0.1 mm/h. The maximum wind-driven load during the monitoring period was 0.95 mm/hr, which is about one-seventh of the horizontal rain that was recorded in the same rain event on November 10. The hourly average and daily total horizontal global solar radiation that were calculated based on the measured data (1 minute sampling period) are presented in Figure 5.

Indoor Climatic Conditions. The indoor temperature and relative humidity conditions of the BETF were controlled by thermostat and humidistat, respectively. The temperature set point was 21°C and was kept constant throughout the monitoring period, as shown in Figure 6. Although it was possible to control the indoor relative humidity during the winter, as can be seen in Figure 6, the indoor relative humidity during the summer period was considerably higher than the set point of 40%. This is due to the fact that the ventilation fan was continuously running and there was no dehumidification unit to remove the excess moisture. Moreover, moisture removal by the air-conditioning unit might have been limited due to the mild outdoor temperature and part-load operation of the equipment, which generally happens in mild, wet climates like Vancouver.

BRIEF DESCRIPTION OF THE ADVANCED HYGROTHERMAL MODEL: HAMFIT

The HAMFit model has two versions, HAMFit-1D and HAMFit2D, to simulate one- and two-dimensional heat, air, and moisture responses of building envelope components, respectively. In this paper, the one-dimensional HAMFit-1D (Tariku et al. 2008; Tariku et al. 2010) was used to simulate the hygrothermal responses of a prefabricated wall system with EPS insulation as exposed to Vancouver weather conditions (Figures 3 to 5) on the outside and controlled indoor climatic conditions in the inside (Figure 6). HAMFit is a transient model with the capability of handling nonlinear and coupled heat, air, and moisture (HAM) transfer processes through multilayered porous media. It takes into account the nonlinear hygrothermal properties of materials, moisture transfer by vapor diffusion, capillary liquid water transport, and convective heat and moisture transfers. Moreover, the model accounts for the effect of moisture in the thermal storage and transfer properties of materials as well as the local heating and cooling effects that are generated within the structure due to moisture phase changes (i.e., condensation and evaporation, respectively). The partial differential equations (PDEs) that are implemented in the HAMFit building envelope model are given in Equations 1 to 3.

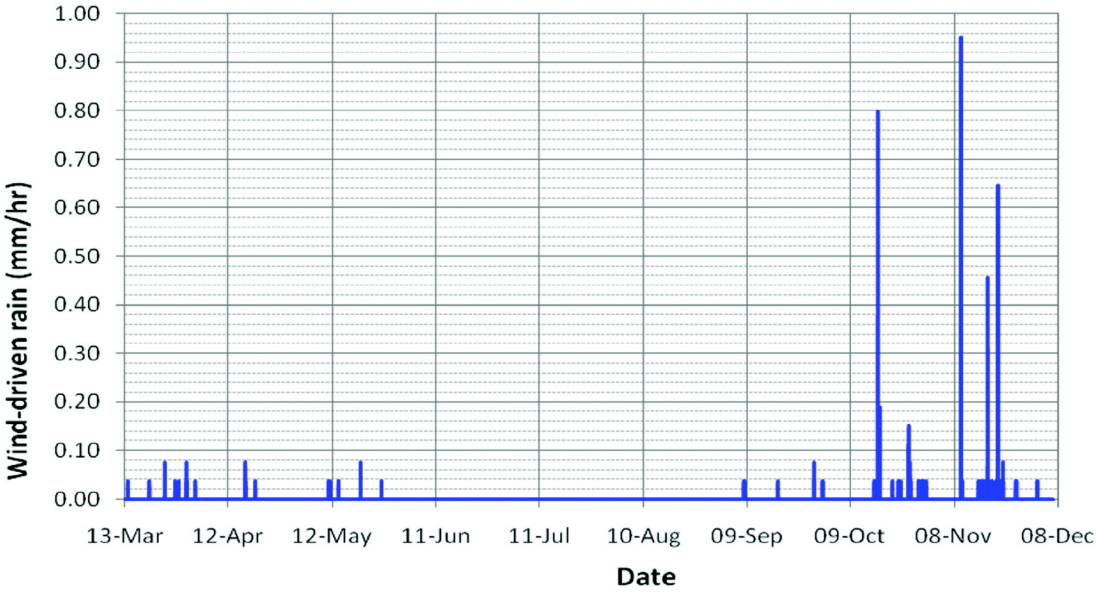

Figure 4 *Hourly wind-driven rain load on test walls during the simulation period.*

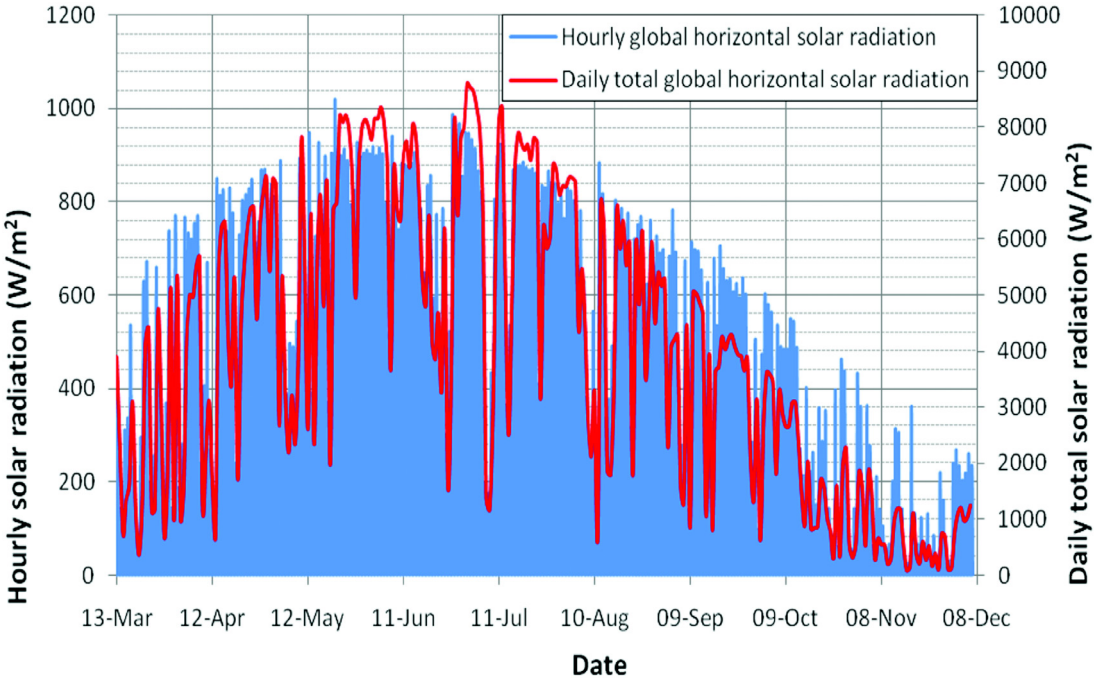

Figure 5 *Hourly average and daily total horizontal global radiation during the simulation period.*

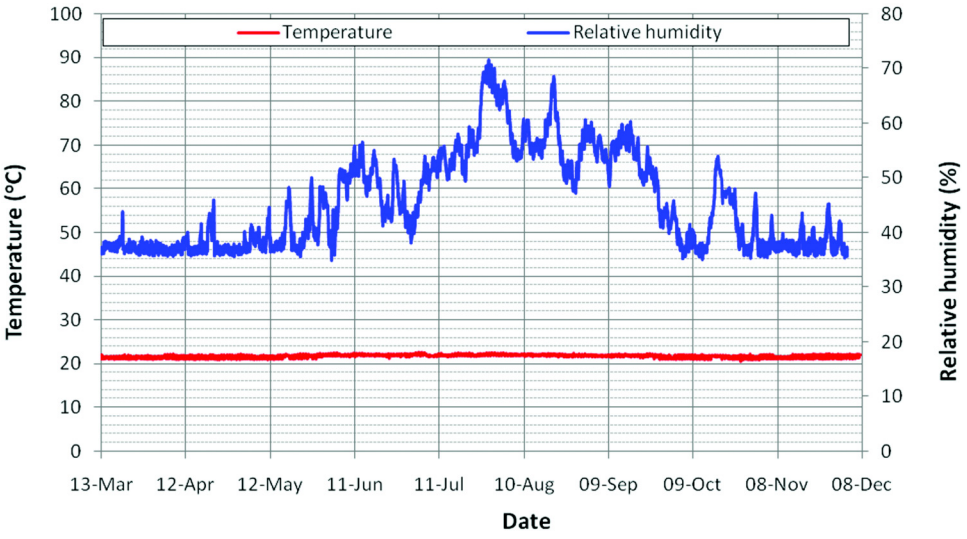

Figure 6 *Indoor temperature and relative humidity of the BETF during the simulation period.*

Moisture Balance

$$\Theta\frac{\partial\phi}{\partial t} = \nabla\cdot(D_\phi\nabla\phi + D_T\nabla T) - \nabla\cdot(D_l\rho_w\vec{g} + \rho_a\vec{u}C_c\widehat{P}\phi) \quad (1)$$

where

$$D_\phi = [\delta_v P + D_l(\rho_w R/M)(T/\phi)],$$

$$D_T = [\delta_v\phi(\partial\widehat{P}/\partial T) + D_l(\rho_w R/M)\ln(\phi)], \quad \text{and}$$

$$C_c = 0.622/P_{atm}.$$

Heat Balance

$$\rho_m Cp_{eff}\frac{\partial T}{\partial t} + \nabla\cdot(\vec{u}T)\rho_a(Cp_a + \omega Cp_v) + \nabla\cdot(-\lambda_{eff}\nabla T) = \dot{m}_c h_{fg} + \dot{m}_c T(Cp_v - Cp_l) + \dot{Q}_s \quad (2)$$

where

$$Cp_{eff} = Cv_m + Y_l Cp_l,$$

$$\lambda_{eff} = \lambda_{dry}C_\lambda, \quad \text{and}$$

$$\dot{m}_c = \nabla\cdot(\delta_v\nabla P_v) - \rho_a\nabla\cdot(\vec{u}\omega).$$

Momentum Balance (Darcy Flow)

$$-\nabla\cdot\left(\rho_a\frac{k_a}{\mu}\nabla P\right) = 0 \quad (3)$$

In HAMFit-1D, the PDEs presented in Equations 1 to 3 are reduced to Equations 4 to 6, where x is the direction perpendicular to the wall.

$$\Theta\frac{\partial\phi}{\partial t} = \frac{\partial}{\partial x}\left(D_\phi\frac{\partial\phi}{\partial x} + D_T\frac{\partial T}{\partial x}\right) - \frac{\partial}{\partial x}(D_l\rho_w\vec{g} + \rho_a\vec{u}C_c\widehat{P}\phi) \quad (4)$$

$$\rho_m Cp_{eff}\frac{\partial T}{\partial t} + \frac{\partial}{\partial x}(\vec{u}T)\rho_a(Cp_a + \omega Cp_v) + \frac{\partial}{\partial x}\left(-\lambda_{eff}\frac{\partial T}{\partial x}\right) = \dot{m}_c h_{fg} + \dot{m}_c T(Cp_v - Cp_l) + \dot{Q}_s \quad (5)$$

$$-\frac{d}{dx}\cdot\left(\rho_a\frac{k_a}{\mu}\frac{dP}{dx}\right) = 0 \quad (6)$$

where ϕ is the relative humidity; Θ is sorption capacity (kg/m^3), T is temperature (°C); δ_v and D_l are the vapor permeability and liquid conductivity of the material (s); P_v, $\widehat{P}$, and P_{atm} are vapor pressure, saturated vapor, and atmospheric pressure (Pa), respectively; R and M are the universal gas constant (8.314 J·K^{-1}·mol^{-1}) and molecular weight of water molecule (0.1806 kg·mol^{-1}), respectively; ρ_a is air density (kg/m^3); ρ_w is density of water (kg/m^3); $\vec{g}$ is the acceleration due to gravity (m/s^2); $\vec{u}$ is air velocity (m/s); ρ_m is density of material (kg/m^3); Cp_a, Cp_v, and Cp_l are the specific heat capacity of air, vapor, and liquid water (J/[K·kg]), respectively; ω is absolute humidity (kg/kg-air); Cp_{eff} and λ_{eff} are the effective specific heat capacity and thermal conductivity (which take moisture effect into account), respectively; Cv_m and λ_{dry} are the heat capacity and thermal conductivity of the material at dry state; C_λ is thermal conductivity correction factor for moisture (determined through experiment); Y_a and Y_l are the air and liquid water mass fractions; $\dot{Q}_s$ is a heat source (or sink) term; h_{fg} is the latent heat of condensation/evaporation (J/kg); $\dot{m}_c$ is the amount of moisture condensation/evaporation (kg/s); and k_a and μ are the airflow coefficient and dynamic viscosity, respectively.

The driving potentials of moisture and heat balance equations (Equations 1 and 2) are relative humidity and tempera-

ture, respectively. Airflow through the porous media is governed by the Darcy equation, which relates the flow rate with pressure gradient and air permeability characteristics of the media (Equation 3). These nonlinear and coupled PDEs are solved simultaneously for temperature, relative humidity and airflow velocity fields across the computational domain (multilayered building envelope component) for a given outside environmental condition (weather data) and prescribed indoor conditions using the finite-element-based commercial software called COMSOL Multiphysics and MatLab. The development and benchmarking of this simulation tool are described in detail in Tariku et al. (2010).

SIMULATION PARAMETERS

The main input parameters that are required to simulate the dynamic response of the wall system are the indoor and outdoor boundary conditions, hygrothermal properties of materials, and initial temperature and moisture conditions of the layers. These parameters are described in detail below.

Boundary Conditions

The boundary conditions that are applied on the interior and exterior surfaces of the computational domain are Neumann-type boundary conditions, where moisture and heat fluxes are used instead of surface temperature and relative humidity conditions (Dirichlet-type boundary conditions). In this paper, the heat and moisture fluxes at the interior surface are calculated from the indoor climatic data, which are presented in Figures 3 to 6, and heat and mass transfer coefficients. The heat transfer coefficient is estimated to be 8 W/(K·m^2) (IEA 1991, 1996), and the mass transfer coefficient of the corresponding surface, 5E-8 s/m, is estimated based on Lewis relation (ASHRAE 2005). The heat transfer coefficient accounts for both convection and long-wave radiation heat exchanges. The external surface is exposed to the local weather conditions of Vancouver. The ambient temperature, relative humidity, solar radiation, and wind-driven loads that are measured and used to determine the hourly moisture and heat fluxes in the simulation are presented in Figures 4 and 5.

The effective heat flux on the exterior surface is calculated by adding the heat gain due to solar radiation and the net heat exchange between the surfaces and the surrounding environment due to long-wave radiation and convective heat exchange mechanisms. Since the exterior convective heat transfer coefficient value depends on wind speed, a variable heat transfer coefficient that is approximated by Equation 7 (Sanders 1996) is used in the simulation. The long-wave radiation heat exchange is estimated based on European Standard prEN ISO/FDIS 13791:2004, Annex E. The model allows using a constant convective heat transfer coefficient or a combined heat transfer coefficient for the convective and long-wave radiation heat fluxes. The exterior surface mass transfer coefficient is determined similar to the indoor surface mass transfer coefficient using the Lewis relation.

$$\begin{aligned} h_c^o &= 5.82 + 3.96V \qquad V \le 5 \text{ m/s} \\ h_c^o &= 7.68V^{0.75} \qquad V > 5 \text{ m/s} \end{aligned} \tag{7}$$

where V is the wind speed measured at 10 m adjacent to the house.

Material Properties

To solve the mathematical equations of heat, air and moisture balance equations described above (Equations 1 to 3), the respective storage and transport properties of the materials need to be defined. In this work, the heat and moisture storage properties heat capacity and sorption isotherm (and water retention), the two moisture transport properties of vapor permeability and liquid diffusivity, and the thermal conductivity of the layers of the materials are taken from ASHRAE Research Project RP-1018 (Kumaran et al. 2002). Table 1 shows the thickness, density, conductivity λ_{dry}, and heat capacity Cv_m of the materials at dry state. In the same table, the vapor permeability δ_v of the materials as a function of relative humidity, and the equilibrium moisture contents (EMC) of the gypsum, plywood, and fiber cement boards at 50% RH and 90% RH are provided. The sheathing board that is used in the experiment is a 12.5 mm thick Douglas fir plywood with a density of 463 kg/m^3. For the simulation, the hygrothermal property data set of "Plywood 2" in ASHRAE Research Project RP-1018 was adopted, as it is Douglas fir and has the same thickness and density as the one used in the experiment. The moisture storage capacity, heat capacity, liquid permeability, and thermal resistance of the polyethylene and sheathing membrane were assumed to be negligible, and values of 0.80 and 0.90, respectively, were assumed for the absorptivity and the emissivity of the dark fiber-cement cladding surface.

Initial Conditions

The additional input data that are required to simulate the transient hygrothermal responses of a building envelope component are the initial hygrothermal conditions of the component. The simulation period starts on March 13, 2009, so the hygrothermal conditions of the wall system at that time that are inferred from the experimental data were used for establishing initial conditions for the simulation. The temperature and moisture content readings of the plywood at the middle section were 13.6°C and 16.7%, respectively. The measured cladding and drywall surface temperatures were 12.8°C and 20°C, respectively. In the simulation, the initial temperature gradient across the insulation was defined using the temperatures of the adjacent layers (i.e., plywood and drywall temperatures). The initial moisture conditions of the cladding and the drywall were estimated based on the moisture conditions of the sheathing board and indoor air, respectively, more specifically under the assumption that these layers will have relative humidities that are similar to the respective adjacent layers. Using the sorption-isotherm curve of the plywood and indoor air measurement data, the initial moisture condi-

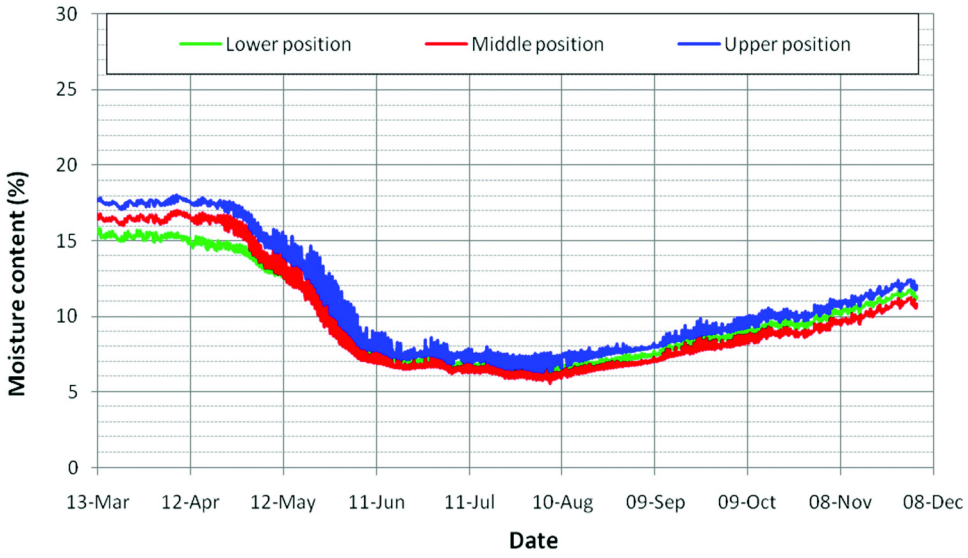

Figure 7 *Moisture content profiles of the sheathing board (plywood) at the lower, middle, and upper positions.*

Table 1. Properties of Materials Used in the Simulation

Materials	Thickness, mm	Density, kg/m^3	Cv_m, J/(kg·K)	λ_{dry}, W/(m·K)	δ_v, kg/(m·s·Pa); ϕ between 0 and 1	EMC at ~50% RH, kg/kg	EMC at ~90% RH, kg/kg
Gypsum drywall	12.5	625	870	0.1600	3E-11 $e^{08745\phi}$	0.004	0.018
Polyethylene sheet	0.15	840	1256	0.1600	4.7E-16	—	—
EPS	102	14.8	1470	0.0379	3E-12 $e^{0.8234\phi}$	—	—
Plywood	12.5	470	1880	0.0858	2E-13 $e^{4.2063\phi}$	0.070	0.158
30 min paper	0.22	909	1880	0.1600	3E-10 $e^{3.039\phi}$	—	—
Fiber cement	7.94	1380	840	0.2500	1E-13 $e^{5.3963\phi}$	0.040	0.168

tions of the cladding and the drywall were set to 90% RH and 45% RH, respectively. The sheathing membrane was assumed to have the same initial temperature and relative humidity conditions as that of the sheathing board (plywood). For modeling purpose, the stated initial temperature and moisture conditions were assumed to be uniformly distributed across the layers thickness, except the insulation layer, where a temperature gradient across the layer was assumed.

Modeling Assumptions

Since the test panel was prefabricated in a manufacturing plant, the vapor/air barrier (polyethylene sheet) installed behind the gypsum board was assumed to be continuous. Subsequently, in the modeling, airflow through the test panel was assumed to be negligible. The wall system was assumed to be with no deficiency, and no wind-driven rain penetration was considered. The layers of materials were assumed to be in perfect contact and exhibit no physical dimensional change with time. The material properties used in the simulation were assumed to represent the materials used in the experiment.

RESULTS AND DISCUSSION

The wall system considered in this study was exposed to Vancouver climatic conditions on the outside and controlled indoor conditions in the inside, which are presented in Figures 3 to 6. The sheathing board was the critical layer in the wall system that was susceptible to moisture damage due to high moisture accumulation. Thus, the transient moisture content and temperature measurement results of the plywood were used to compare with HAMFit's simulation results of the same wall.

Figure 7 shows the measured moisture content profiles of the sheathing board at the upper, middle and lower sections. As shown in the figure, in the first two months, the plywood was in a slow drying process. During this period, the indoor temperature and relative humidity were relatively stable at

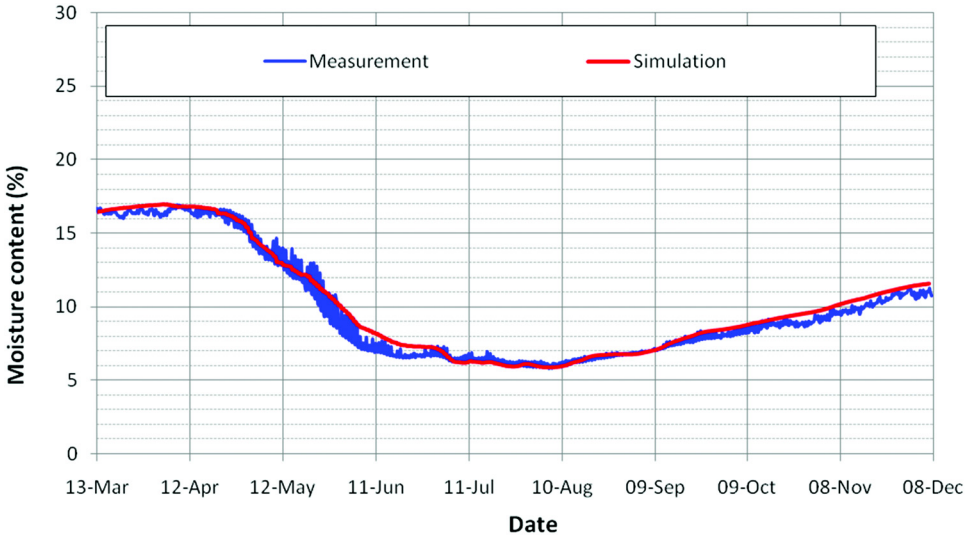

Figure 8 *Transient moisture content profile of the plywood as simulated using HAMFit.*

21°C and 36%, respectively, and the exterior surfaces of the walls were exposed to 10 wind-driven rain events (all under 0.1 mm/h), higher outdoor relative humidity, and low solar radiation, which might have contributed to slow drying of the sheathing board. The drying process accelerated in May as the ambient temperature and solar radiation increased. The moisture content changes in the plywood during the summer months of June and July were limited. This is expected since the plywood was relatively dry and further drying was a very slow process. During this period, the ambient temperature and solar radiation as well as the indoor relative humidity were rather high, and there were no wind-driven rain events. Moisture transfer between the indoor and outdoor air was limited due to the presence of low-vapor-permeance layers (i.e., the 6 mil polyethylene sheet and EPS insulation) behind the interior layer (gypsum board). The moisture content of the plywood started to increase at the beginning of August and continued to the end of the reporting period. The plywood's moisture content increase in the fall season resulted from the reduction in the ambient temperature and solar radiation, which reduced the plywood temperature, coupled with the presence of relatively humid air.

As can be seen in Figure 7, the moisture content profiles of the three locations (upper, middle, and lower sections) were similar, with the middle section bounded by the lower and upper sections profiles. For the monitoring period considered here, the maximum moisture content deviation among the three is less than 2%, which is within the accuracy range of the moisture pin measurement system. Since there is no significant moisture content difference among the three sections of the plywood, the heat and moisture transport through the wall system can be considered as a one-dimensional transport process. Subsequently, in this work, the one-dimensional version of the HAMFit model is used for simulation and comparison purposes.

Figure 8 shows the transient moisture content profile of the plywood as simulated using the hygrothermal model, HAMFit. For comparison purposes, the experimental result obtained from the moisture pin measurement is superimposed on the figure. The simulation started on March 13, 2009, and ran for a continuous period of 272 days. The drying curve that was generated through the simulation has the same trend and is in good agreement with the experimental result. During the entire monitoring period, deviations between the simulation and measurement results were all under 2% moisture content (MC). The higher deviations occurred during the spring season. In the first week of May, the experimental result shows faster drying process of plywood than the simulation suggests, which subsequently results slightly higher moisture content prediction till the end of June. The higher drying rate might be the result of extra moisture removal from the wall by airflow through the gap between the sheathing membrane and the cladding, which is not taken into account in the one-dimensional modeling. In the summer and fall, the simulation and the experimental results are in very good agreement.

The hygrothermal model, HAMFit, outputs spatial and temporal variations of temperature and relative humidity within the computational domain. Figure 9 shows the transient moisture content profiles at the outer, middle, and inner sections of the plywood, which are 3 mm, 6.5 mm, and 3 mm thick, respectively. The drying curves of the three sections that are generated through the simulation have the same trend. As the simulation results indicate, there is more moisture gradient across the plywood thickness during the drying period, April 24 to August 8 as well as in the fall, when the wetting process initiated. During these periods, the inner section of the plywood is slow to dry and also slow to accumulate moisture

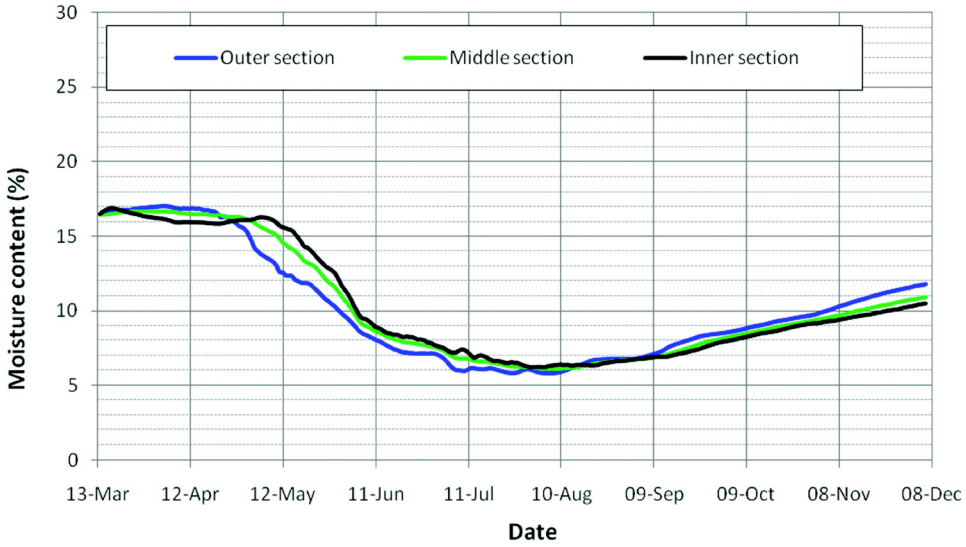

Figure 9 *Moisture content profiles of plywood at the outer, middle, and inner sections of the plywood.*

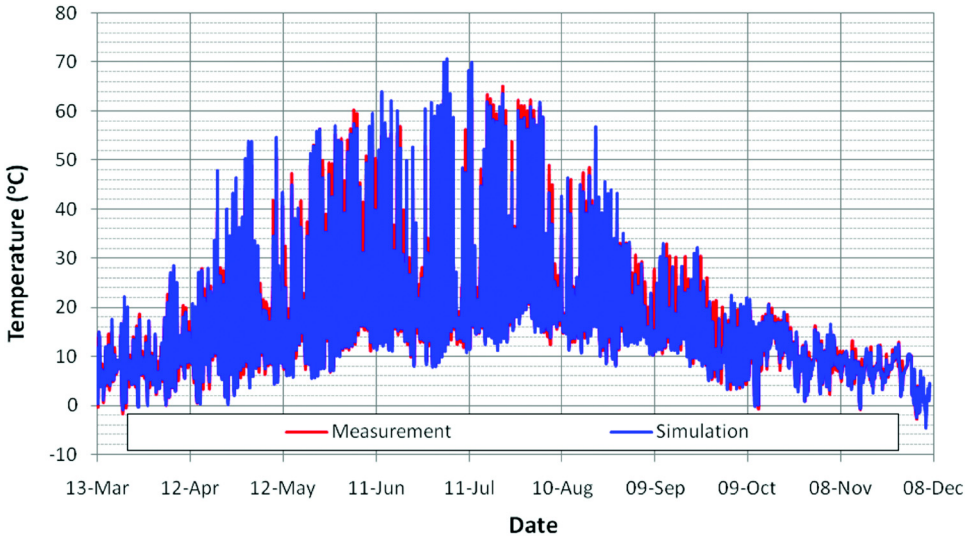

Figure 10 *Hourly average interior surface temperature of the plywood as obtained from measurement and simulation.*

during the drying and wetting periods, respectively, since moisture movement to and from the indoor space is significantly reduced by the vapor barrier and the rigid insulation.

Figure 10 shows the hourly average interior surface temperature of the plywood as obtained from the experimental as well as simulation results. As can be seen from the figure, the hygrothermal simulation shows similar dynamic temperature responses as the measurement. In general, the simulation results are in good agreement with measured values. For the entire simulation period, deviations between the simulation and experimental values were under 2°C for 70% of the time (6528 data points) and under 5°C for 90% of the time. The higher deviations were observed during the summer period and when solar radiation dominated the heat transfer process. This is because, in the simulation, the solar radiation flux on the exterior surface is derived from the measured global horizontal solar radiation using an empirical relation, which is sometimes different from the actual solar radiation that the exterior surface of the test wall receives. In general, the thermal response of the plywood is sensitive to the solar radiation flux. Figure 11 shows the measured and calculated daily average temperature of the interior surface of the plywood, which shows good agreement between the two. During the monitoring period, the daily average surface temperature of the plywood varies from the lowest value of 0°C on December 6 to 33.6°C on July 29.

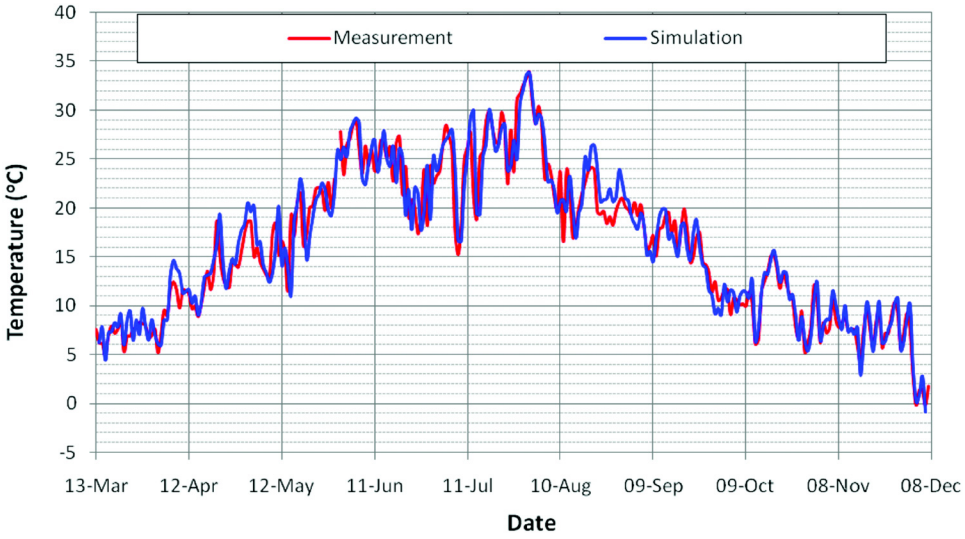

Figure 11 *Daily average interior surface temperature of the plywood as obtained from measurement and simulation.*

CONCLUSION

In this paper, the hygrothermal response of a sheathing board in a prefabricated wall system, which is exposed to the outdoor Vancouver weather and controlled indoor climatic conditions, was modeled and compared with measured data. As the experimental results suggest, the moisture content differences among the top, middle, and low sections of the sheathing board were minimal. This is mainly attributed to the wall system's configuration where the natural convection loop, which is responsible for variation of temperature and moisture content across the vertical section of a sheathing board in a wall system with batt insulation, is eliminated due to the presence of a rigid insulation in the cavity. Moreover, heat and moisture transport by airflow across the wall system are significantly reduced by the rigid insulation (EPS), 6 mil polyethylene, and good workmanship. In general, the heat and moisture transfer through the wall system considered in this study can be characterized as a one-dimensional transport process. Both simulation and measurement results show faster drying of the sheathing board during the spring season. The simulation shows a moisture gradient across the sheathing board, and its direction is mainly linked to the outdoor climate. The good agreement obtained between the simulation and the experimental results validates the advanced hygrothermal model, HAMFit, and demonstrated its capability. The model is useful to assess the hygrothermal performance of wall systems, as it can provide detailed spatial and temporal hygrothermal conditions of building envelope components.

ACKNOWLEDGMENTS

The authors would like to acknowledge the financial support received from the School of Construction and the Environment, British Columbia Institute of Technology, and Pacific Building Systems, and the assistance of Stephen Roy and Wendy Simpson.

REFERENCES

ASHRAE. 2009. *2009 Handbook—Fundamentals*. Atlanta, GA: American Society of Heating, Refrigeration and Air-Conditioning Engineers, Atlanta

Baker, M.C. 1969. Decay of wood. *Canadian Building Digest* 111:4.

Carll, C.G. and T.L. Highley. 1999. Decay of wood and wood-based products above ground in buildings. *Journal of Testing and Evaluation* 27(2):150–58.

Djebbar, R., D. van Reenen, and F. Tariku. 2002. *Hygrothermal performance of building envelope retrofit options; Task 3a—Hygrothermal performance analysis of high-rise masonry wall assemblies.* Research Report, NRC Institute for Research in Construction.

Ge, H., R. Krpan, P. Fazio, and Y. Ye. 2008. A two-storey field station for investigation of building envelope performance in the coastal climate of British Columbia. *Proceedings of the Symposium in Building Physics*, Leuven, Belgium.

Ge, H., F. Tariku, and S. Roy. 2009. *Field evaluation of the thermal and moisture performance of Pacific Building Systems' Smart Wall Systems*. Technical report submitted to Pacific Building Systems.

Geving, S. and S. Uvsløkk. 2000. *Test house measurements for verification of heat-, air and moisture transfer models*. Norwegian Building Research Report No. 273, Trondheim, Norway.

Hagentoft, C-E., A. Kalagasidis, B. Adl-Zarrabi, S. Roels, J. Carmeliet, H. Hens, J. Grunewald, M. Funk, R. Becker, D. Shamir, O. Adan, H. Brocken, K. Kumaran, and

R. Djebbar. 2004. Assessment method of numerical prediction models for combined heat, air and moisture transfer in building components: Benchmarks for one-dimensional cases. *Journal of Thermal Envelope and Building Science* 27(4):327–52.

IEA. 1991. *Sourcebook, Annex 14: Final report, vol. 1*. International Energy Agency, Leuven, Belgium.

IEA. 1996. *Heat, air and moisture transfer through new and retrofitted insulated envelope parts, Annex 24: Final report, vol. 2, Task 2: Environmental conditions*. International Energy Agency, Leuven, Belgium.

ISO. 2004. *European Standard prEN ISO/FDIS 13791:2004, Thermal performance of buildings—Calculation of internal temperatures of a room in summer without mechanical cooling—General criteria and validation procedures.* International Organization for Standardization.

Kumaran, K., J. Lackey, N. Normandin, F. Tariku, and D. van Reenen. 2002. *A thermal and moisture transport property database for common building and insulating materials, final report—ASHRAE Research Project 1018-RP.* Atlanta, GA: American Society for Heating, Refrigerating and Air-Conditioning Engineers, Inc.

Maref, W., M.A. Lacasse, M.K. Kumaran, and M.C. Swinton. 2002. Benchmarking of the advanced hygrothermal model-hygIRC with mid-scale experiments. *eSim 2002 Proceedings*, University of Concordia, Montreal, pp. 171–76.

Maref, W., F. Tariku, and B. Di Lenardo. 2009. Hygrothermal performance of exterior wall systems using an innovative vapour retarder in Canadian climate. *4th International Building Physics Conference*, Istanbul.

Mukhopadhyaya, P., M.K. Kumaran, F. Tariku, and D. van Reenen. 2003. *Final report from task 7 of MEWS project at the Institute for Research in Construction: Long-term performance: Predict the moisture management performance of wall systems as a function of climate, material properties, etc. through mathematical modelling*. Research Report RR-132, NRC Institute for Research in Construction.

Nofal, M. and P.I. Morris. 2003. Criteria for unacceptable damage on wood systems. *Japan-Canada Conference on Building Envelope*, Vancouver, pp. 1–14.

Tariku, F. and M.K. Kumaran. 2006. Hygrothermal modeling of aerated concrete wall and comparison with field experiment. *Proceedings of the 3rd International Building Physics/Engineering Conference*, Montreal, pp. 321–28.

Tariku, F., S. Cornick, and M. Lacasse. 2007. Simulation of wind-driven rain effects on the performance of a stucco-clad wall. *Proceedings of Thermal Performance of the Exterior Envelopes of Whole Buildings X International Conference*, Clearwater, FL.

Tariku, F., M.K. Kumaran, and P. Fazio. 2008. Development and benchmarking of a new hygrothermal model. *11th International Conference on Durability of Building Materials and Components*, Istanbul, pp. 1413–20.

Tariku, F., M.K. Kumaran, and P. Fazio. 2010. Transient model for coupled heat, air and moisture transfer through multilayered porous media. *International Journal of Heat and Mass Transfer* 53(15–16):3035–44.